

Tailored Preparation Methods of TiO₂ Anatase, Rutile, Brookite: Mechanism of Formation and Electrochemical Properties[†]

Damien Dambournet,* Ilias Belharouak,* and Khalil Amine

Chemical Sciences and Engineering Division, Argonne National Laboratory, 9700 South Cass Avenue,
Argonne, Illinois 60439

Received August 24, 2009. Revised Manuscript Received November 3, 2009

Using a simple aqueous precipitation method based on a low-cost titanium oxysulfate precursor, we have prepared three TiO₂ polymorphs: anatase, rutile, and brookite. Although the anatase form can be directly obtained from the thermolysis reaction of an oxysulfate solution, the rutile and the brookite have been prepared by the addition of oxalate species. Depending on the concentration, the oxalate anions have been shown to act either as a ligand with the stabilization of a titanium oxalate hydrate, Ti₂O₃(H₂O)₂(C₂O₄)·H₂O, or as a chelating agent with the isolation of the rutile phase. The brookite form was obtained by thermal decomposition of the oxalate hydrate at a temperature as low as 300 °C. The resulting solid consisted of nanodomains of TiO₂ brookite embedded in large micrometer-size particles and exhibited a high specific surface area of 255 m²/g because of the mesoporosity arising from the removal of water from the oxalate species. This type of morphology is of interest for lithium-ion batteries because of an easier coating process and a higher surface contact between the material and the electrolyte that enhanced the electrochemical activity. Finally, based on electrochemical characterizations, TiO₂ brookite provided higher volumetric energy density than comparable nanomaterials.

1. Introduction

Beyond their wide use in small electronic devices, lithium-ion batteries are now facing the challenge of meeting the energy and power requirements for plug-in hybrid vehicles and electric vehicles. Research has been focused on the development of new electrode materials that could provide higher power, longer cycle life, lower cost, and enhanced safety. With regard to the negative electrode, the mechanism of lithiation of carbonaceous materials is governed by the formation of a solid-electrolyte interface (SEI) layer generated after reduction of the electrolyte species. This SEI layer enables the reversibility of lithium-ion insertion, leading to a high energy density. However, it is thermally unstable and therefore poses safety concerns. These concerns are allayed by operating at a higher voltage than that of metallic lithium, which prevents the decomposition of the electrolyte. Titanium oxide (titania) is an interesting alternative anode¹ to graphite because of its operating voltage (~1.5 V), which may enable extended cycle life as well as enhanced safety. Additionally, titanium is abundant, nontoxic, and inexpensive. These characteristics are of great importance with regard to the production of batteries in large scale. However, the practical capacity (~170–200 mA h/g)

achieved by the TiO₂ anode is much lower than the theoretical one (335 mA h/g) based on the full electrochemical activation of the Ti⁴⁺/Ti³⁺ redox couple and still needs to be sustained over long-term cycling. This capacity stability can be achieved by the use of nanostructured titania materials. Indeed, nanomaterials have attracted significant attention in the energy storage and conversion field owing to their specific features² that enhance the electrochemical activity so that full lithium ion reversibility can be achieved. Nevertheless, in addition to low volumetric energy density, the need for the large-scale production of nanomaterials can be argued to be disadvantageous for Li-ion batteries, because their preparation can be very complex² and can add tremendously to the cost of the final battery pack.

Since the 1970s, the so-called “chimie douce” has introduced synthetic methods that lead to new materials with unique features, including the synthesis of hybrid materials or the low temperature synthesis of oxides.³ The precipitation process in aqueous solutions is one of the synthetic methods developed through the “chimie douce.” This process has been used to prepare titanium oxide compounds with easy control of the size/morphology as well as the structural arrangement.⁴ The latter advantage is relevant since titanium dioxide has several allotropic forms with different structures. The most

[†] Accepted as part of the 2010 “Materials Chemistry of Energy Conversion Special Issue”.

*Corresponding author. E-mail: dambournet@anl.gov (D.D.); belharouak@anl.gov (I.B.).

(1) Deng, Da; Kim, Min Gyu; Lee, Jim Yang; Cho, Jaephil *Energy Environ. Sci.* **2009**, 2, 818.

(2) Arico, A. S.; Bruce, P. G.; Scrosati, B.; Tarascon, J.-M.; Schalkwijk, W. V. *Nat. Mater.* **2005**, 4, 366.

(3) Livage, J. *New J. Chem.* **2001**, 25, 1.

(4) Jolivet, J. P.; Cassaignon, S.; Chaneac, C.; Chiche, D.; Tronc, E. *J. Sol-Gel Sci. Technol.* **2008**, 46, 299.

well-known are rutile (tetragonal, $P4_2/mnm$), anatase (tetragonal, $I4_1/amd$), and brookite (orthorhombic, $Pbca$).⁵ Their structures are all built upon the connection of TiO_6 octahedra. Although the anatase structure consists of edge-sharing TiO_6 octahedra, the rutile and the brookite frameworks exhibit both corner- and edge-sharing configurations (Figure 1). These phases can be prepared in an aqueous medium.⁶ Nevertheless, because of the metastability of the brookite form, its preparation appears to be more challenging. To the best of our knowledge, only two methods have been reported on the aqueous precipitation of pure TiO_2 brookite. Potier et al.⁷ prepared it by the thermolysis reaction of $TiCl_4$ in concentrated HCl, followed by peptization with concentrated nitric acid. The other method is the oxidation of $TiCl_3$ in an aqueous solution containing urea.⁸ Because of the difficulty in preparing this TiO_2 polymorph, only a few studies^{9–12} have been devoted to its use as an anode for lithium ion-batteries, as opposed to the anatase and rutile phases, which have been extensively studied.

In this paper, we report on isolating the three above-mentioned TiO_2 polymorphs by using the chimie douce tools. A mechanism for their formation is proposed, and their electrochemical activity is characterized.

2. Experimental Procedure

The synthesis process consisted of the thermolysis of titanium oxysulfate (Sigma Aldrich, Supelco) in an aqueous solution with a concentration of 0.9 M. First, $TiOSO_4$ is dissolved in water by slight heating. The precipitation of TiO_2 is then performed by heating the solution at 90 °C for 4 h. The powder is recovered by centrifugation (4000 rpm) or filtration, and then washed with water. To ensure the TiO_2 stoichiometry, we performed thermogravimetric analysis to define an appropriate post-treatment annealing. In a second step of this investigation, this synthesis was performed in the presence of different anionic species through the use of lithium salt additives, i.e., $LiNO_3$, $LiCl$, Li_2SO_4 , and $Li_2C_2O_4$ (Sigma Aldrich). To do so, we dissolved the lithium and titanium salts simultaneously.

The prepared samples were analyzed by various methods. Powder X-ray diffraction analysis was performed with a Siemens D5000 diffractometer (Cu $K\alpha$). The samples were scanned from $2\theta = 10$ – 80° at a scan rate of 5 s per 0.02° . Scanning electron microscopy (SEM, Hitachi S-4700-II) was performed at the Electron Microscopy Center at Argonne National Laboratory. Thermogravimetric analysis (TGA) was performed with a Seiko Exstar 6000 instrument at a scan rate of 5 °C/min in the temperature range of room temperature to 800 °C. Differential

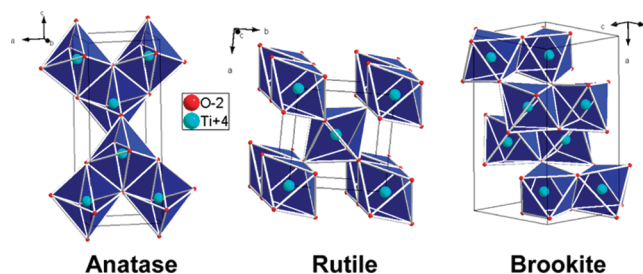


Figure 1. Representations of the TiO_2 anatase, rutile, and brookite forms.

scanning calorimetry (DSC) analysis was conducted with a Perkin-Elmer Pyris-1 instrument. The DSC curves were recorded between room temperature and 400 °C at a scan rate of 5 °C/min. An empty stainless-steel capsule was used as a reference pan.

Nitrogen adsorption isotherms were recorded at 77 K on a NOVA 2200e instrument. The powder sample (~200 mg) was evacuated at 200 °C for 2 h prior to N_2 adsorption. The total pore volume was calculated from the volume of nitrogen adsorbed at relative pressure of $P/P^0 = 0.986$. The specific surface area was calculated from the BET method applied in the P/P^0 range between 0.04 and 0.29. The pore size distribution was obtained by means of the Barrett–Joyner–Halenda algorithm using the adsorption branch.

Electrochemical measurements were carried out with CR2032-type coin cells. The negative electrodes were made of 80 wt % active oxide materials, 10 wt % acetylene black as the conductive agent, and 10 wt % polyvinylidene difluoride binder. The electrolyte was 1.2 M $LiPF_6$ dissolved in a (3:7 volume ratio) mixture of ethylene carbonate and ethyl methyl carbonate. The cells were assembled with lithium metal as the negative electrode and were tested in the voltage range of 1–3 V.

3. Results and Discussion

3.1. Synthesis and Structural Characterizations.

3.1.1. Thermolysis of an Aqueous Oxysulfate Solution. Most TiO_2 synthesis has involved the use of titanium chloride or alkoxide precursor. In the present paper, we used a titanium oxysulfate-sulfuric acid complex hydrate ($TiOSO_4 \cdot H_2O \cdot H_2SO_4$) as a precursor, which is a low cost salt and, as opposed to other titanium salts, is easy to handle. As a starting point, the thermolysis reaction of an aqueous titanium oxysulfate solution was studied without anionic species additives. The presence of sulfuric acid in the starting precursor induced a strong acidic medium with a pH value of 0.1. TiO_2 was precipitated at 90 °C after 4 h of reaction. The resulting powder exhibits agglomerates of nanosize particles whose X-ray diffraction pattern is that of TiO_2 anatase (Figure 2). This result suggests that sulfate species act as a directing agent that favors the formation of anatase at the expense of the thermodynamically stable phase, i.e., the rutile form. In general, in an aqueous medium, titanium cations are solvated and form 6-fold-coordinated, charged complexes $[TiL_6]^{z+}$ in which the nature of the ligand L is dictated by the pH of the solution and the presence of species that can act as complexing agents.¹³ In the absence

- (5) *Inorganic Crystal Structure Database*, version 2009-1; Fachinformationszentrum Karlsruhe: Karlsruhe, Germany, 2009.
- (6) Jolivet J. *Sol–Gel Sci. Technol.* **2008**, *46*, 299.
- (7) Potier, A.; Chaneac, C.; Tronc, E.; Mazerolles, L.; Jolivet, J. P. *J. Mater. Chem.* **2001**, *11*, 1116.
- (8) Li, J.-G.; Tang, C.; Li, Di; Haneda, H.; Ishigaki, T. *J. Am. Ceram. Soc.* **2004**, *87*(7), 1358–1361.
- (9) Anji Reddy, M.; Satya Kishore, M.; Pralong, V.; Varadaraju, U. V.; Raveau, B. *Electrochem. Solid-State Lett.* **2007**, *10*(2), A29–A31.
- (10) Anji Reddy, M.; Pralong, V.; Varadaraju, U. V.; Raveau, B. *Electrochem. Solid-State Lett.* **2008**, *11*(8), A132–A134.
- (11) Lee, D. H.; Park, J. G.; Choi, K. J.; Choi, H. J.; Kim, D. W. *Eur. J. Inorg. Chem.* **2008**, 878.
- (12) Lee, D.-H.; Park, J.-G.; Choi, K. J.; Choi, H.-J.; Kim, D.-W. *Cryst. Growth Des.* **2008**, *8*, 12.

- (13) Jolivet, J. P. *Metal Oxide Chemistry and Synthesis: From Solution to Solid State*; Wiley: New York, 2000.

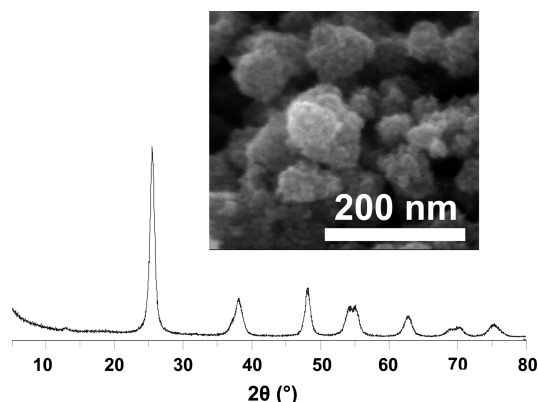


Figure 2. X-ray diffraction powder pattern of TiO_2 anatase obtained from the thermolysis of an oxysulfate solution. Inset: Scanning electron microscopy image of the solid.

of complexing ligand, acidity plays a major role. For instance, in high acidic medium, because of the polarizability of Ti^{4+} ions, the complex $[\text{Ti}(\text{H}_2\text{O})_6]^{4+}$ undergoes a spontaneous hydroxylation reaction, forming the $[\text{Ti}(\text{OH})(\text{H}_2\text{O})_5]^{3+}$ complex. Further hydroxylation reactions lead to the formation of a zero-charge complex with the following formula: $[\text{Ti}(\text{OH})_4(\text{H}_2\text{O})_2]^0$. These reactions can be promoted by either adding a base (coprecipitation process) or heating the solution (thermolysis process). By condensation reactions, this complex can result in the formation of a solid phase through the creation and growth of the nuclei. This process is based on ololation and oxalation reactions. In the presence of complexing agents that can react with the coordination sphere of the cation, the solid phase is likely to form from different zero-charge precursors, leading to the stabilization of one particular phase. In our case, sulfate species play the role of the complexing agents and can enter the coordination sphere of Ti^{4+} ions. Koelsh et al.,¹⁴ indeed, proposed the existence of the following zero-charge precursor: $[\text{Ti}(\text{OH})_2\text{SO}_4(\text{H}_2\text{O})_2]^0$, where SO_4^{2-} ions act as bidentate ligands. More recently, the speciation of titanium(IV) in sulfuric acid solutions has shown the occurrence of $1\text{Ti}:1\text{SO}_4$ and $1\text{Ti}:2\text{SO}_4$ species, with the predominance of the 1:1 complex.¹⁵ These complexes exist in low amounts, suggesting their role as a catalyst or structure-directing agent favoring the anatase type structure. According to Jolivet,¹³ the formation of sulfate species in the vicinity of the cation may favor the condensation of opposed coplanar edges, leading to the anatase configuration.

To further probe the effect of additional species in solution, experiments were performed with anionic species having different complexing strength: SO_4^{2-} , NO_3^- , and Cl^- . The molar ratio between Ti^{4+} and the additional anionic species was fixed at one. X-ray diffraction analysis, shown in Figure 3, was used to probe the effect of these species. The sulfate species improved the crystallinity of the prepared phase, which confirmed their pro-

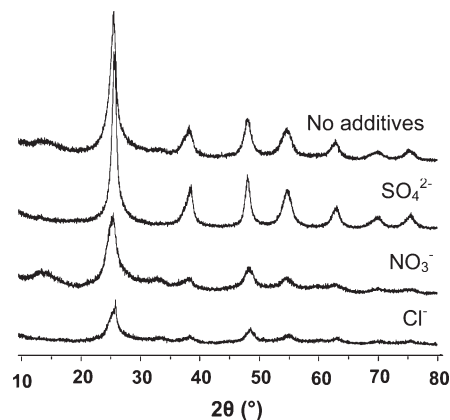


Figure 3. X-ray diffraction powder pattern of the TiO_2 anatase obtained from the thermolysis of an oxysulfate solution with and without the addition of different anionic species.

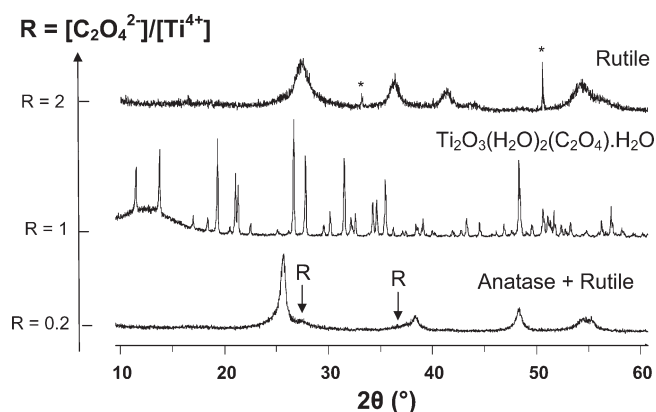


Figure 4. X-ray diffraction powder pattern as a function of the $R = [\text{C}_2\text{O}_4^{2-}]/[\text{Ti}^{4+}]$ molar ratio (* sample holder).

moting role. In contrast, the addition of the chloride anion, a strong complexing agent, led to a poorly crystallized anatase phase (Figure 3). Chloride anions can enter the first coordination sphere of titanium, forming hydroxochloro complexes. As opposed to sulfate species, the chloride anion favors the formation of the brookite phase after formation of the suggested zero-charge precursor $[\text{Ti}(\text{OH})_2\text{Cl}_2(\text{H}_2\text{O})_2]^0$.⁷ Finally, in the case of nitrate NO_3^- , which is a weak complexing anion, the prepared sample presents a slight decrease in the anatase crystallinity (Figure 3).

3.1.2. Addition of Oxalate Species. The oxalate anion $\text{C}_2\text{O}_4^{2-}$ has been considered for its properties as a rigid bidentate ligand that can link two metallic centers, but also for its chelating properties.¹⁶ To probe the reactivity of the oxalate anion with titanium ions, the $R = [\text{C}_2\text{O}_4^{2-}]/[\text{Ti}^{4+}]$ molar ratio has been tuned. Figure 4 shows the evolution of the powder X-ray diffraction patterns as a function of the $[\text{C}_2\text{O}_4^{2-}]$ content. Three domains were distinguished. A low concentration ($R = 0.2$) yielded a phase mixture consisting of anatase (major phase) and rutile. For $R = 1$, the titanium oxalate-based compound $\text{Ti}_2\text{O}_3(\text{H}_2\text{O})_2(\text{C}_2\text{O}_4) \cdot \text{H}_2\text{O}$ was identified.

(14) Koelsh, M.; Cassaignon, S.; Jolivet, J. P. *Mater. Res. Soc. Symp. Proc.* **2004**, 822, 73.

(15) Szilagy, I.; Konigsberger, E.; May, P. M. *Inorg. Chem.* **2009**, 48, 2200.

(16) Rao, C. N. R.; Natarajan, S.; Vaidyanathan, R. *Angew. Chem., Int. Ed.* **2004**, 43, 1466.

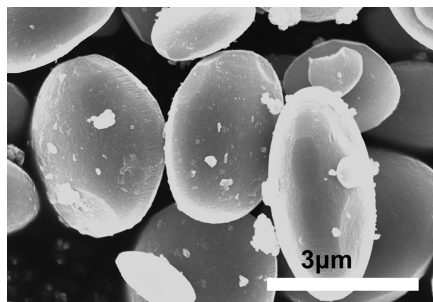


Figure 5. Scanning electron microscopy image of $[\text{Ti}_2\text{O}_3(\text{H}_2\text{O})_2(\text{C}_2\text{O}_4)] \cdot \text{H}_2\text{O}$.

Finally, the higher oxalate content ($R = 2$) yielded an oxide having the rutile-type structure. Depending on the concentration, the oxalate anion can either act as a ligand with the stabilization of an oxalate hydrate phase $\text{Ti}_2\text{O}_3 \cdot (\text{H}_2\text{O})_2(\text{C}_2\text{O}_4) \cdot \text{H}_2\text{O}$ ($R = 1$) or as a chelating agent ($R = 2$) with the stabilization of the rutile phase with a low yield. At first, it was surprising that the increase of the oxalate concentration ($R = 2$) did not favor the formation of the oxalate hydrate $\text{Ti}_2\text{O}_3(\text{H}_2\text{O})_2(\text{C}_2\text{O}_4) \cdot \text{H}_2\text{O}$, but led to the stabilization of an oxide. However, because of the chelating properties of $\text{C}_2\text{O}_4^{2-}$ anions, further complexation of titanium ions by the oxalate ligands inhibits the stabilization of $\text{Ti}_2\text{O}_3(\text{H}_2\text{O})_2(\text{C}_2\text{O}_4) \cdot \text{H}_2\text{O}$ and instead favors the formation of the thermodynamically stable TiO_2 rutile. The blocking effect of the oxalate anions on condensation reaction was also confirmed by the low yield from the reaction, i.e., 30%, which can be enhanced by an increase of the synthesis temperature.

Figure 5 shows a scanning electron micrograph of the $\text{Ti}_2\text{O}_3(\text{H}_2\text{O})_2(\text{C}_2\text{O}_4) \cdot \text{H}_2\text{O}$ compound. This solid consists of 3 μm particles having an eggshell morphology. The structure and composition of this phase have been recently reinvestigated by Boudaren et al.¹⁷ The phase consists of TiO_6 -based layers that are interconnected by oxalate anions, and it crystallizes in an orthorhombic symmetry ($Cmca$). Profile matching (Le Bail method) confirmed the phase purity. The unit cell parameters are in agreement with the literature, i.e., $a = 15.436(3) \text{ \AA}$, $b = 10.421(2) \text{ \AA}$, and $c = 9.692(2) \text{ \AA}$. The chemical composition was confirmed by thermogravimetric analysis (Figure 6, left), which indicated a total weight loss of 43.7% (against 44.1% theoretically). The different steps of the thermal decomposition are related to the dehydration (below 200 $^\circ\text{C}$) and removal of the oxalate species (above 200 $^\circ\text{C}$). The removal of oxalate species occurs in two steps: the formation of a carbonate phase at around 350 $^\circ\text{C}$ and the decomposition of the oxalate to form TiO_2 .¹⁷ Differential scanning calorimetric analysis was also conducted on $\text{Ti}_2\text{O}_3(\text{H}_2\text{O})_2(\text{C}_2\text{O}_4) \cdot \text{H}_2\text{O}$ (Figure 6, right). Two endothermic peaks were detected: a strong peak occurring at 275 $^\circ\text{C}$ and a weak one at 295 $^\circ\text{C}$. Both peaks are related to the removal of the oxalate species. No exothermic event related to the crystallization of TiO_2 has been detected.

$\text{Ti}_2\text{O}_3(\text{H}_2\text{O})_2(\text{C}_2\text{O}_4) \cdot \text{H}_2\text{O}$ has been subjected to different thermal treatment and the corresponding X-ray diffraction pattern is shown in Figure 7. Surprisingly, the titanium oxalate hydrate phase decomposed into the metastable TiO_2 brookite form. Note that because the main diffraction line of the anatase form is close to the one for the brookite form, the thermal decomposition of the $\text{Ti}_2\text{O}_3(\text{H}_2\text{O})_2(\text{C}_2\text{O}_4) \cdot \text{H}_2\text{O}$ had been previously reported to lead to the TiO_2 anatase form.¹⁷ At a temperature as low as 300 $^\circ\text{C}$, the X-ray pattern of the brookite was clearly identified. The broadness of the X-ray lines indicates the formation of nanosized brookite. An increase in the temperature led to an improvement of the crystallinity. At 600 $^\circ\text{C}$, the brookite form started to decompose, with the detection of a tiny peak ascribed to the main diffraction peak of the rutile phase (Figure 7).

In a previous study by Tomita et al.,¹⁸ TiO_2 brookite was also reported to be formed using an organic–inorganic compound, $(\text{NH}_4)_6[\text{Ti}_4(\text{C}_2\text{H}_2\text{O}_3)_4(\text{C}_2\text{H}_3\text{O}_3)_2(\text{O}_2)_4\text{O}_2]$. Nevertheless, this water-soluble titanium complex has to be treated under hydrothermal conditions to form TiO_2 brookite. The facile synthesis and low stability of $\text{Ti}_2\text{O}_3(\text{H}_2\text{O})_2(\text{C}_2\text{O}_4) \cdot \text{H}_2\text{O}$ make it a suitable precursor as part of a simple preparation method for TiO_2 brookite. An additional salient point about this preparation method is the preservation of the morphology upon annealing (Figure 8). As evident from the SEM images, the eggshell morphology is retained despite the creation of porosities arising from the removal of water and oxalate species. This observation has been confirmed by N_2 adsorption (Figure 9). The curve in Figure 9 is typical of a type IV isotherm,¹⁹ which is consistent with mesoporous TiO_2 brookite. The surface area calculated by the BET method was 255 m^2/g , which can only be explained by the existence of significant porosity created at the level of the eggshell micrometer-size particles. The mesopore size was centered at 3.4 nm, and the total porous volume was 0.25 mL/g . Finally, based on the high surface area and porosity numbers associated with the broadness of the diffraction lines, TiO_2 brookite obtained after decomposition of the titanium oxalate hydrate consists of nano-domains embedded in micrometer-size particles.

3.2. Electrochemical Characterization. Figure 10 presents the discharge and charge profiles of the three TiO_2 forms cycled between 1 and 3 V (vs Li^0) at a $C/25$ rate. A “1C” rate here refers to the application of 335 mA/g current density in a cell. The lithium insertion occurs typically at around 1.4–1.7 V according to the following scheme: $x\text{Li}^+ + \text{TiO}_2 + xe^- \leftrightarrow \text{Li}_x\text{TiO}_2$. Such a reaction implies the reduction of Ti^{4+} into Ti^{3+} ions.²⁰ The insertion of one Li^+ ion per unit formula is equivalent to the achievement of the 335 mA h/g theoretical capacity of TiO_2 . During the initial discharge, all three phases

(17) Boudaren, C.; Bataille, T.; Auffrédic, J. P.; Louër, D. *Solid State Sci.* **2003**, *5*, 175.

(18) Tomita, K.; Petrykin, V.; Kobayashi, M.; Shiro, M.; Yoshimura, M.; Kakihana, M. *Angew. Chem., Int. Ed.* **2006**, *45*, 2378.

(19) Brunauer, S.; Emmett, P. H.; Teller, E. *J. Am. Chem. Soc.* **1938**, *60*(2), 309.

(20) Sodergren, S.; Siegbahn, H.; Rensmo, H.; Lindstrom, H.; Hagfeldt, A.; Lindquist, S. E. *J. Phys. Chem., B* **1997**, *101*, 3087.

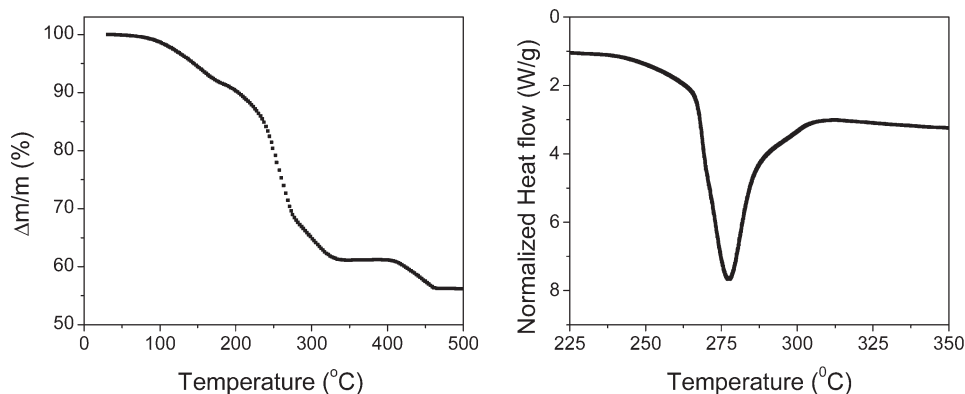


Figure 6. Thermogravimetric (left) and differential scanning calorimetric (right) analyses of $[\text{Ti}_2\text{O}_3(\text{H}_2\text{O})_2](\text{C}_2\text{O}_4) \cdot \text{H}_2\text{O}$.

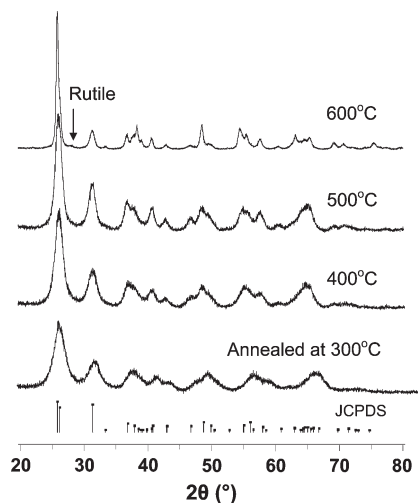


Figure 7. X-ray diffraction analysis of $[\text{Ti}_2\text{O}_3(\text{H}_2\text{O})_2](\text{C}_2\text{O}_4) \cdot \text{H}_2\text{O}$ thermally treated at different temperatures for 4 h under air.

showed capacities close to the theoretical one, i.e., 333 mA h/g (0.99Li^+) for the rutile, 310 mA h/g (0.92Li^+) for the anatase, and 282 mA h/g (0.84Li^+) for the brookite. During the charge (deinsertion), the observed irreversible capacities (31% for anatase, 26% for rutile, and 21% for brookite) are indicative of the lithium ion remaining (0.28Li^+ for anatase, 0.26Li^+ for rutile, 0.18Li^+ for brookite) in the pristine structures. Note that despite the generation of slightly lower capacity, the Coulombic efficiency was higher in the case of TiO_2 brookite.

In general, the lithium insertion in electrode materials can occur in a homogeneous or heterogeneous manner, leading to different structural behavior upon lithiation. Lithium insertion can indeed proceed via single-phase solid-solution behavior or two-phase structural transition. The voltage profile (Figure 10) accounts for the structural behavior upon lithiation. During the first discharge, the brookite exhibits a smooth curve, indicating a solid-solution behavior. On the contrary, both anatase and rutile display a much more complex discharge profile, with the existence of plateau zones that likely account for the coexistence of biphasic domains. For the rutile form, except the first discharge, further charge/discharge processes indicate single-phase reversible behavior. For the first discharge, two plateau zones are observed, at 1.4 and 1.1 V, which were

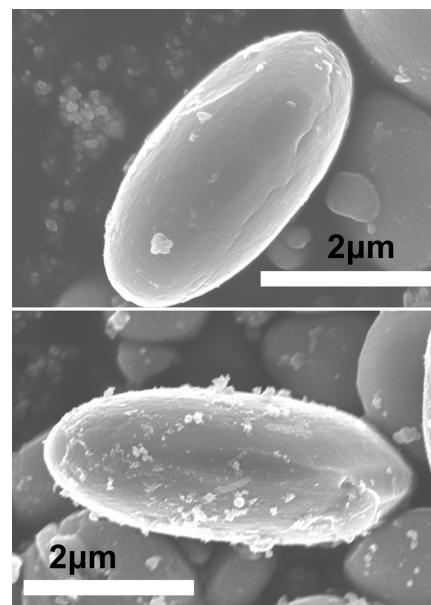


Figure 8. Scanning electron microscopy images of $[\text{Ti}_2\text{O}_3(\text{H}_2\text{O})_2](\text{C}_2\text{O}_4) \cdot \text{H}_2\text{O}$ (top image) and TiO_2 brookite (bottom) obtained by thermal decomposition at 300°C .

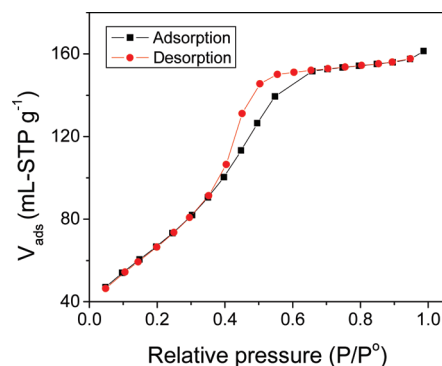


Figure 9. N_2 adsorption isotherms of TiO_2 brookite prepared by thermal decomposition of $[\text{Ti}_2\text{O}_3(\text{H}_2\text{O})_2](\text{C}_2\text{O}_4) \cdot \text{H}_2\text{O}$ at 300°C .

ascribed to a structural rearrangement upon lithiation, from the original rutile $P4_2/mmm$ to its lithiated form $P2_1/m$ at 1.4 V and finally to a layered structure at 1.1 V.²¹ The last plateau leads to a drastic and irreversible structural

(21) Borghols, W. J.; Wagemaker, M.; Lafont, U.; Kelder, E.; Mulder, F. M. *Chem. Mater.* **2008**, *20*, 2949.

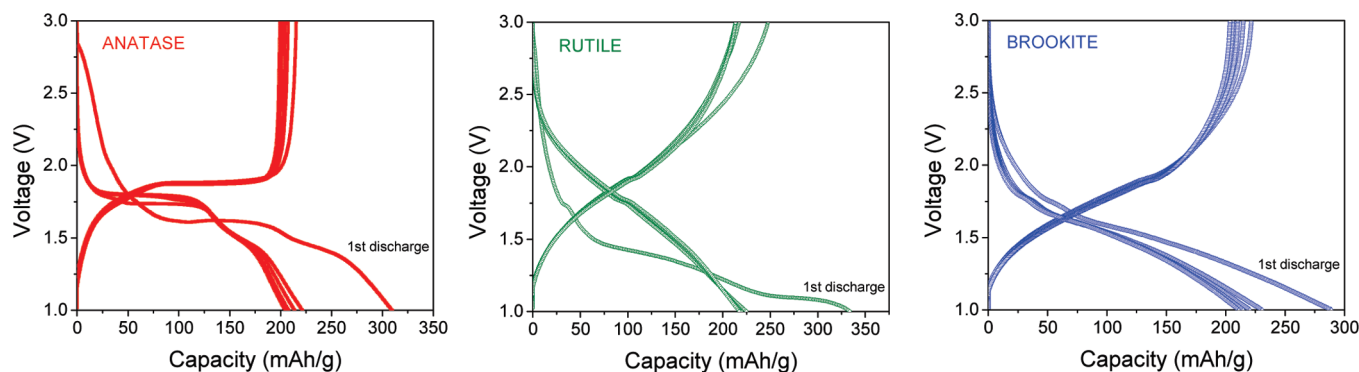


Figure 10. Voltage profile of the different TiO_2 forms cycled at $C/25$.

change, which explains the single-phase insertion/extraction profile after the first discharge. This behavior has only been observed for nanosized rutile.²² As for the anatase, bulk crystallites display a two-phase transition profile characterized by a flat plateau zone related to the coexistence of a Li-poor phase, $\text{Li}_{0.05}\text{TiO}_2$, having the anatase original space group, i.e., $I4_1/amd$, and a Li-rich phase $\text{Li}_{0.5}\text{TiO}_2$ ($Imma$).²³ For nanosized particles, in addition to the Li-rich phase, the anatase type structure can behave as a solid solution with the insertion of up to 1 Li^+ ion per TiO_2 .²⁴ The brookite was found to present a partial amorphization upon lithiation,⁹ so that it was difficult to probe structural changes. Nevertheless, upon lithium removal, the phase can recover its initial crystallinity in agreement with single-phase behavior. Research is underway to fully elucidate the structural behavior of the brookite upon lithiation.

Because of its originality in term of morphology, further electrochemical characterizations have been performed on the TiO_2 brookite form (Figure 11). This type of morphology is indeed of interest for lithium-ion batteries for several reasons. First, in terms of electrode fabrication, spherical-type particles exhibit a better dispersibility suitable during the coating process of the material on the current collector. Second, the mesoporosity provides a higher surface contact between the material and the electrolyte, which enhances the electrochemical activity.²⁵ Finally, this type of morphology can provide high volumetric energy density in a battery. For instance, most nanomaterials dedicated to Li-ion battery applications suffer from low packing density, which despite the enhancement of their electrochemical performances compromises the overall energy density of the battery. In our case, the titanium oxalate hydrate provides a tap density of 1.2 g/cm^3 , which slightly decreases upon annealing, to 1.05 g/cm^3 . The cyclability of TiO_2 brookite performed under a $C/15$ rate is presented in Figure 11. Both gravimetric (mA h/g) and volumetric (mA h/cm^3) capacities are reported. The

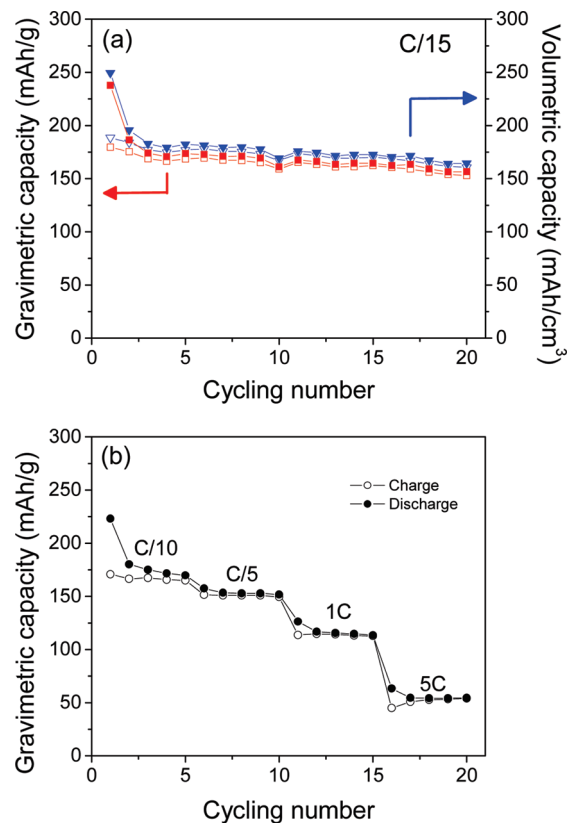


Figure 11. (a) Gravimetric and volumetric capacity of TiO_2 brookite under $C/10$ (33.5 mA/g); (b) rate capability of TiO_2 brookite.

volumetric capacity has been calculated from the product of the gravimetric capacity and tap density. TiO_2 brookite showed a stable cycling behavior with the retention of 155 mA h/g after 20 cycles. Such a value is in the range of those found for nanosize brookite.¹⁰ The volumetric capacity was around 165 mA h/cm^3 , which is significantly higher than most nanosized TiO_2 materials because the latter display lower packing density, i.e., $0.5\text{--}0.8 \text{ g/cm}^3$.

The evolution of the capacity of TiO_2 brookite with increasing rates has been also studied and is displayed in Figure 11. TiO_2 brookite exhibited a specific discharge capacity of 170 mA h/g under $C/10$ rate which reduced to 152 , 113 , and 55 mA h/g at $C/5$, $1C$ and $5C$ rates, respectively. Such a decrease of capacity while increasing the current density can be ascribed to the insulating

- (22) Hu, Y.-S.; Kienle, L.; Guo, Y.-G.; Maier, J. *Adv. Mater.* **2006**, *18*, 1421.
- (23) Wagemaker, M.; Kearley, G. J.; van Well, A. A.; Mutka, H.; Mulder, F. M. *J. Am. Chem. Soc.* **2003**, *125*, 840.
- (24) Wagemaker, M.; Borghols, W. J. H.; Mulder, F. M. *J. Am. Chem. Soc.* **2007**, *129*, 4323.
- (25) Guo, Y. G.; Hu, Y. S.; Maier, J. *Chem. Commun.* **2006**, 2783.

character of TiO_2 . There are, however, several ways to improve the electronic conductivity of insulating materials including the use of conductive additives such as glassylike phases,²⁶ carbon²⁷ or metal²⁸ coating, or design of hierarchical network.²⁹ Future works are thus underway to improve the rate capability of TiO_2 brookite and will be reported elsewhere.

4. Conclusion

The investigation of the thermolysis reaction of a titanium oxysulfate with and without the presence of additives has been shown to be very rich through the preparation of three different forms of TiO_2 , which are the anatase, rutile, and brookite. Because of its ability to react with the coordination shell of the Ti^{4+} ions, the promoting effect of sulfate (SO_4^{2-}) species toward the anatase form has been confirmed. The supplemental addition of anionic species such as NO_3^- or Cl^- led to the anatase form exhibiting different crystallinity depending on the ability of the anion to react with Ti^{4+} ions in solution. For instance, for a chloride anion having a strong complexing strength, the prepared solid consisted of an ill-crystalline anatase phase. Further investigating the use of additives for the preparation of TiO_2 , oxalate species ($\text{C}_2\text{O}_4^{2-}$) have been considered because of its strong complexing properties. Increasing the $R = [\text{C}_2\text{O}_4^{2-}]/[\text{Ti}^{4+}]$ molar ratio led to the successive isolation of the titanium oxalate hydrate $\text{Ti}_2\text{O}_3(\text{H}_2\text{O})_2(\text{C}_2\text{O}_4) \cdot \text{H}_2\text{O}$ ($R = 1$) and the rutile phase ($R = 2$). The isolation of the TiO_2 rutile using high concentration of oxalate emphasized the chelating properties of this anion. A detailed

investigation of the thermal behavior of the $\text{Ti}_2\text{O}_3(\text{H}_2\text{O})_2(\text{C}_2\text{O}_4) \cdot \text{H}_2\text{O}$ has shown that it decomposes into the TiO_2 brookite form at a temperature as low as 300 °C. The resulting solid consisted of nanodomains of TiO_2 brookite embedded in large micrometer-size mesoporous particles and exhibited a very high specific surface area of 255 m^2/g because of the mesoporosity. The electrochemical properties of the three phases were characterized in a lithium cell configuration. The cell tests showed that all phases approached the theoretical capacity (335 mA h/g) of one lithium ion insertion in TiO_2 for the first discharge. Except for certain differences in voltage profiles that are due to the basic differences in the lithium insertion mechanism among the three structural frameworks, the operating voltage of the anatase, rutile, and brookite phases is about 1.7 V, with most of the capacity being achieved above 1 V. Within this voltage region, most electrolytes are electrochemically very stable, and combining these lithium insertion materials with higher potential materials, such as LiMn_2O_4 or $\text{LiNi}_{0.5}\text{Mn}_{1.5}\text{O}_4$, would result in battery systems with better life and safety. Moreover, this work has shed light on the electrochemical properties of the TiO_2 brookite phase; such data are scarce in the literature. Our experimental procedure has established a new facile method to prepare the metastable brookite phase. The high packing density particles built from nanosize crystallites associated with a high surface area because of the porosity makes this morphology, unique and suitable for a large scale production and its use as electrode material. Even with slightly lower capacity compared to anatase or rutile, brookite's high volumetric capacity is of great importance if the phase is to be used in full-scale batteries.

Acknowledgment. This research was funded by the U.S. Department of Energy, FreedomCAR and Vehicle Technologies Office. Argonne National Laboratory is operated for the U.S. Department of Energy by UChicago Argonne, LLC, under Contract DE-ACO2-06CH11357.

- (26) Zhou, H. S.; Li, D. L.; Hibino, M.; Honma, I. *Angew. Chem., Int. Ed.* **2005**, *44*, 797.
- (27) Fu, L. J.; Liu, H.; Zhang, H. P.; Li, C.; Zhang, T.; Wu, J. P.; Holze, R.; Wu, H. Q. *Electrochem. Commun.* **2006**, *8*, 1.
- (28) Mancinia, M.; Kubiaka, P.; Geserick, J.; Marassi, R.; Hüsing, N.; Wohlfahrt-Mehrens, M. *J. Power Sources* **2009**, *189*, 585.
- (29) Guo, Y.-G.; Hu, Y.-S.; Sigle, W.; Maier, J. *Adv. Mater.* **2007**, *19*, 2087.